

Ünal Akdağ · Mustafa Özdemir

## Heat transfer in an oscillating vertical annular liquid column open to atmosphere

Received: 12 January 2005 / Accepted: 5 September 2005 / Published online: 8 October 2005  
© Springer-Verlag 2005

**Abstract** The heat transfer from a surface heated with constant heat flux to an oscillating vertical annular liquid column having an interface with the atmosphere is investigated experimentally in the present paper. The analysis is carried out for the case of different oscillation frequencies while the displacement amplitude remains constant. Based on the experimental data a correlation equation is obtained for the cycle-averaged Nusselt number as a function of kinetic Reynolds number.

**Keywords** Oscillating interface · Heat transfer · Annular duct

### Nomenclature

$A$  Cross-sectional area of liquid column ( $\text{m}^2$ )  
 $A_o$  Dimensionless oscillation amplitude  
 $A_p$  Cross-sectional area of piston ( $\text{m}^2$ )  
 $c$  Specific heat of fluid ( $\text{kJ/kg-K}$ )  
 $d$  Hydraulic diameter of test duct (m)  
 $h$  Heat transfer coefficient ( $\text{W/m}^2\text{-K}$ )  
 $H_1, H_2$  Cycle-averaged enthalpies (J)  
 $L$  Total distance from probe1 to probe2 (m)  
 $l_h$  Heater length (m)  
 $l_o$  Distance from probes to heater (m)  
 $Pr$  Prandtl Number  
 $Q_k$  Total heat loss to environment over a cycle (J)  
 $Q_l$  Total heat transferred to water over a cycle (J)  
 $q_e$  Total wall heat flux (W)  
 $q_1''$  Heat flux from heater to control volume ( $\text{W/m}^2$ )  
 $q_2''$  Heat flux from glass tube to environment ( $\text{W/m}^2$ )  
 $R$  Flywheel radius (m)  
 $Re_\omega$  Kinetic Reynolds number  
 $r_1$  Inner radius of annulus (m)

$r_2$  Outer radius of annulus (m)  
 $x_m$  Oscillation amplitude (m)  
 $t$  Time (s)  
 $T$  Temperature  
 $T_a$  Ambient temperature ( $^\circ\text{C}$ )  
 $T_b$  Bulk temperature ( $^\circ\text{C}$ )  
 $T_{ca}$  Temperatures of the outer surface of glass tube corresponding to air region of the test section ( $^\circ\text{C}$ )  
 $T_{cl}$  Temperatures of the outer surface of glass tube corresponding to water region of the test section ( $^\circ\text{C}$ )  
 $T_{10}$  First probe temperatures ( $^\circ\text{C}$ )  
 $T_{20}$  Second probe temperatures ( $^\circ\text{C}$ )  
 $T_{wo}$  Space-cycle averaged wall temperatures ( $^\circ\text{C}$ )  
 $T_0$  Averaged bulk temperature defined in 14 ( $^\circ\text{C}$ )  
 $u$  Mean velocity (m/s)  
 $u_m$  Maximum velocity (m/s)  
 $y$  Vertical coordinate  
 $y^*$  Distance from reference to the meniscus (m)  
 $z$  Interface position (m)  
 $z_0$  Oscillation axis or filling height (m)

### Greek Symbols

$\delta$  Momentum boundary layer thickness (m)  
 $\phi$  Loss parameter defined in (8)  
 $\rho$  Fluid density ( $\text{kg/m}^3$ )  
 $\omega$  Angular frequency (rad/s)

### Subscripts

l Liquid  
a Air

Ünal Akdağ (✉) · M. Özdemir  
Mechanical Engineering Faculty, Istanbul Technical University,  
34437 Gumussuyu, Istanbul, Turkey  
E-mail: akdagun@itu.edu.tr  
Tel.: +90-212-2931300  
Fax: +90-212-2450795

## 1 Introduction

Heat and mass transfer in oscillating flow are fundamental investigation fields in recent years. Oscillation-induced heat transport processes maintain an effective

heat enhancement comparable with heat pipes. It has many important applications in the compact heat exchangers, cooling processes of nuclear plants, design of Stirling heat machines and heat transport in internal combustion machines.

Chatwin [1] and Watson [2] among many others have discussed mass transfer in pulsating and oscillating flow, in order to understand transport phenomena in respiratory and circulatory organs of the human body. They investigated the axial contaminant dispersion in harmonic variation of axial pressure gradient. And they presented that the axial contaminant dispersion increased by oscillation. Based on the analogy between heat and mass transfer, Kurzweg [3–4] investigated the longitudinal heat transfer process in laminar oscillation flow inside a tube bundle which was jointed to a hot reservoir on the upper side and a cold reservoir at the bottom. They showed that the longitudinal heat transfer was increased by laminar oscillation flow to the levels similar to that of heat pipes. The kind of heat transfer process studied by Kurzweg is also called dream pipe, because the heat transfer in oscillating flow is remarkably increased depending on the amplitude and frequency.

Ozawa and Kawamoto [5] investigated the heat transfer mechanism experimentally and numerically on a similar setup by using thermal flow visualization. In their study, they pointed out that the longitudinal heat transfer was increased by means of the phase lag between the boundary and bulk regions of the fluid. Zhao and Cheng [6] have given an extensive literature survey on the heat and mass transfer in pulsating and oscillating flow. Zhao and Cheng [7] carried out an experimental and numerical study for forced convection in a long heated pipe subjected to uniform heat flux with a laminar reciprocating flow of air. They obtained a

correlation equation for the cycle-averaged Nusselt number. Zhao and Cheng [8] also investigated numerically the heat transfer for laminar forced convection of a periodically reversing flow in a pipe heated at constant temperature. They recommended four similarity parameters such as Prandtl number, kinetic Reynolds number, dimensionless oscillation amplitude and the length to diameter ratio of the heated tube. Tang and Cheng [9] obtained a correlation equation for cycle-averaged Nusselt number in terms of Reynolds number, kinetic Reynolds number and dimensionless fluid displacement by a multivariate statistical analysis.

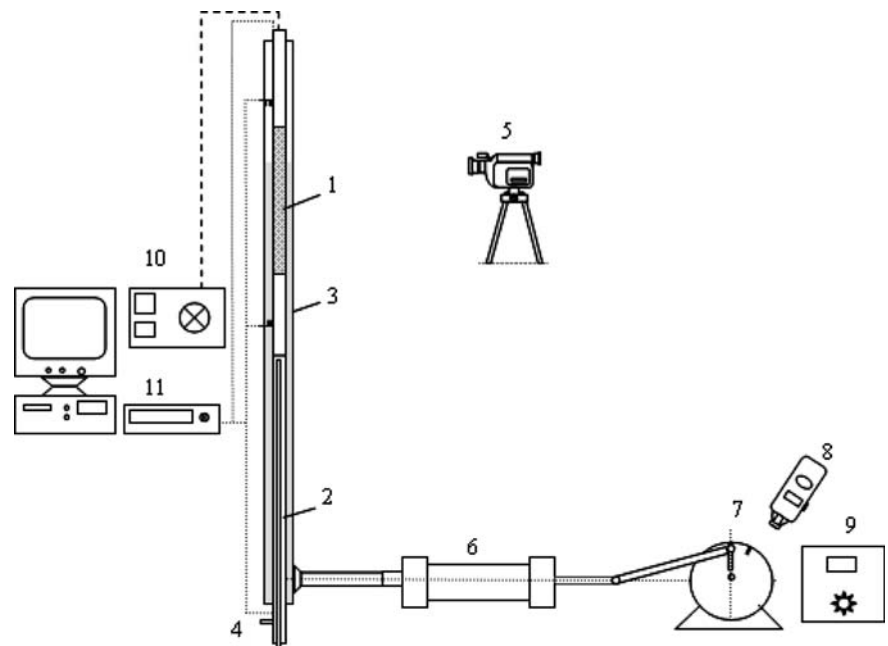
The heat transfer from a discrete heat source on a vertical wall near an oscillating gas/liquid interface has been investigated experimentally by Chen and Chen [10]. They recommended an empirical equation for average Nusselt number based on Reynolds number and Prandtl number in the case of oscillating interface without evaporation.

This study reports part of an extensive research on the heat transfer from a surface heated with constant heat flux to an oscillating vertical annular liquid column having an interface with the atmosphere, experimentally. The analysis is carried out for different oscillation frequencies while the displacement amplitude remains constant for all the cases considered. In the experiments, the heated surface temperature is kept low enough to prevent water from evaporation. A correlation equation is obtained for the cycle-averaged Nusselt number as a function of kinetic Reynolds number.

## 2 Experimental setup

Figure 1 is a schematic diagram illustrating the apparatus of the experimental setup. The outer part of the

**Fig. 1** Experimental setup, 1 Heater, 2 Cooler, 3 Glass pipe, 4 Cooling water inlet and outlet, 5 Camera 6 Piston-cylinder apparatus, 7 DC Motor, 8 Dijital tachometer, 9 Velocity control, 10 Power supply, 11 Data acquisition system (Keitley-2700)



vertical annular test section is a glass tube 2 m in length, 42 mm in outer diameter and 37.4 mm in inner diameter. A cylinder 18 mm in outer diameter consisting of four zones such as heater, cooler and adiabatic parts, is located at the centerline of the glass tube. The heater and cooler are made of copper tubes with lengths of 600 and 760 mm, respectively, while the adiabatic parts 300 mm in length are made of Teflon. One of the adiabatic parts is placed between heater and cooler. The other one which is located on the top of the heater is in the shape of a hollow tube in order to house the cables of the heater. The axial heat conduction of Teflon cylinder and tube is negligible compared with the copper ones. These four zones are assembled together using threaded joints in order to obtain smooth continuums surface.

The heater is built by embedding an electrical resistance inside the copper tube. The cables of six thermocouples located at the inner surface of the heater tube are taken out of the test section by passing them inside of the heater tube and the adiabatic Teflon tube above the heater. Thus, the flow disturbances which might have resulted from caused power and thermocouple cables are eliminated. Since thermocouple cables are located parallel to the electrical cables DC power is used to feed the heater in order to prevent thermocouples from electrical inductance.

The cooler is made of two concentric copper tubes. The cooling water enters the inner tube which is 8 mm in diameter and leaves from the outer tube of the cooler. Seven thermocouples are welded on the cooler surface and the leads are taken out of the test section by passing them through the cooling water.

The first temperature probe is located at the half of the adiabatic section between heater and cooler in order to measure the water temperature and to determine the enthalpy of the flow. This location is also the reference position to measure the positions of the surface temperatures and the interface. This first probe consisting of four thermocouples located different positions across the annular gap. The second probe is the same as first one and it is positioned at 150 mm above the heater section. Each thermocouple signal of the probes is recorded and then the probe temperatures are calculated by averaging the thermocouple signals over the cross-sectional area.

The outer surface temperatures of the glass tube are also measured by five thermocouples. All thermocouples are calibrated using a constant temperature bath to ensure the surface temperatures. A computer controlled data acquisition system (Keithley 2700) is used to collect data. The reciprocating motion of the water column is created using a piston-cylinder driven by a 1 kW DC motor with adjustable speed. The number of revolutions of the motor is measured by an optical digital tachometer (Lutron DT-2234B).

The filling height of the water column is kept constant for all the cases ( $z_0 = 625$  mm). The experiments are conducted at three different heating powers and four different radial frequencies.

### 3 Results and discussion

#### 3.1 Liquid column velocity

It is observed that the motor frequency measured by tachometer is the same as the frequency of the recorded motion of the interface.

While the maximum uniform velocity of the water column is  $R\omega A_p/A = u_m$  as function of piston cross-sectional area, water column cross-sectional area, flywheel radius and frequency, the variation of the mean velocity of the liquid column with time can be written as follows.

$$u(t) = u_m \sin \omega t \quad (1)$$

It can be assumed that the interface is a flat surface by neglecting the capillary and wall effects. Then, the height  $z$  which shows the approximate position of the interface is derived easily as follows by integration of 1.

$$z(t) = z_0 - x_m \cos \omega t \quad (2)$$

Here,  $x_m = RA_p/A$  (amplitude of  $z$ ) and  $z_0$  is the oscillation axis as shown in Fig. 2.

#### 3.2 Surface and fluid temperatures

While the oscillation axis of the water column is always in the heater section, the heater area swept by water is increased and decreased in turn by oscillation. The contact period of water and air to the heater varies harmonically depending on the frequency. Therefore, variation of the heater section temperatures versus time also oscillates depending on the frequency as shown in Fig. 3. The amplitudes of the temperatures at  $\omega = 1.4346$  rad/s decrease when the radial frequency is  $\omega = 2.7227$  rad/s. While increasing frequency decreases the surface temperatures, it disorders the harmonic variation because of shaking. On the other hand, the amplitudes of the heater surface temperatures in the air section decrease at two frequencies considered above, and the smooth harmonic variation is disordered. This can be caused by the water film on the wall.

The time-averaged heater surface temperatures vary with position as shown in Fig. 4. While the averaged temperatures increase with increasing  $y$  in the water section, they remain approximately constant or decrease slightly in the air section, because of the free falling effect of the water film on the heater wall.

The variation of the area-averaged probe temperatures with time is shown in the Fig. 5. The amplitude of the air side probe temperature is lower than the water side probe temperature. While the air temperature decreases, the water temperature increases as shown in the figure. There is a phase lag of approximately  $180^\circ$  between the probe temperatures.

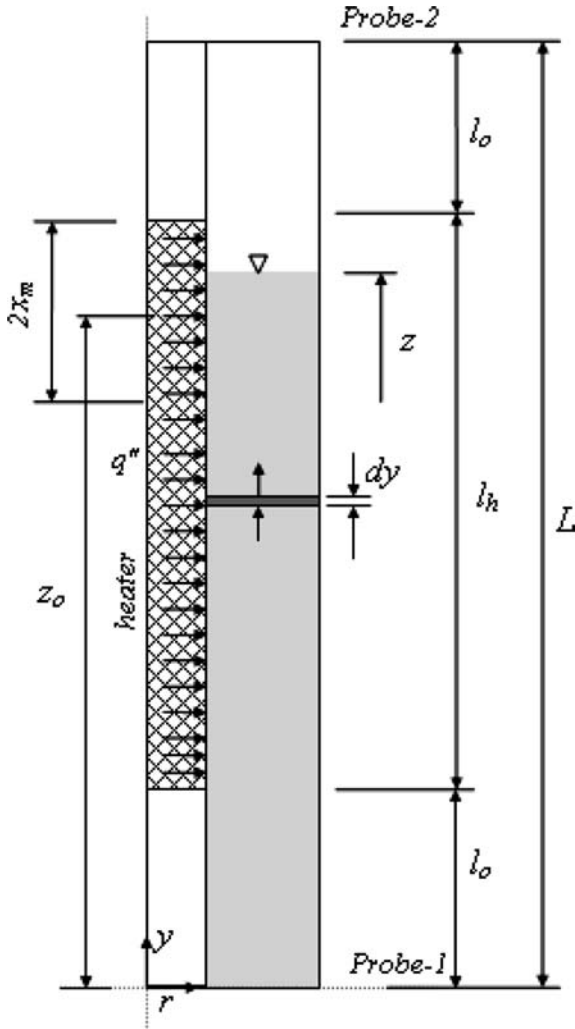


Fig. 2 Control volume between two probes and dimensions

### 3.3 Calculation of the cycle-averaged heat transfer

The region that the inertial and viscous forces in the flow domain are equal is in the order of  $\sqrt{2\nu/\omega}$ . The momentum diffusion decreases quickly away from the wall. The penetration depth that senses the wall effects is approximately given by Zhao and Cheng [6] as follows.

$$\delta \cong 3\sqrt{2\nu/\omega} \quad (3)$$

This depth is below 1 mm for the frequencies considered in this study. Thus, the velocity profile can be assumed uniform in the annular channel. The thermal energy equation in the case of neglected the viscous dissipation and heat conduction in the flow direction ( $y$ -direction) can be written as follows.

$$\frac{\partial T}{\partial t} + u \frac{\partial T}{\partial y} = \alpha \frac{\partial}{\partial r} \left( r \frac{\partial T}{\partial r} \right) \quad (4)$$

By integration of this equation over the cross-sectional area, the following equation is obtained easily.

$$\frac{\partial T_b}{\partial t} + u \frac{\partial T_b}{\partial y} = \frac{2}{\rho c (r_2^2 - r_1^2)} (r_1 q_1'' - r_2 q_2'') \quad (5)$$

Where  $q_1'', q_2''$  are the heat fluxes on the heater surface and the outer surface of the glass tube, respectively. And the bulk temperature is defined by  $T_b = \frac{1}{A} \int T dA$ . The problem analyzed in this study is a conjugate heat transfer problem of the water–air system. The height  $z$  can indicate the position of the water–air interface approximately. In reality the water–air interface is not a flat surface because of the capillary and the water film created by the motion. Thus, the wetted heater surface can not be identified only by the  $z$ -position. Considering the thermal energy conservation given by 4 for water and air regions individually cannot give practical result, since the surface of the interface and the velocity at each point on the interface are unknown. Thus, we consider the thermal energy equation for the whole system consisting of water and air regions together. If the 5 is integrated over the control volume shown in Fig. 2 and integrated over a cycle, we get

$$\begin{aligned} H_2 - H_1 &= \oint u A \rho_a c_a T_{ba}(L, t) dt - \oint u A \rho_1 c_1 T_{bl}(0, t) dt \\ &= q_1'' 2\pi r_1 l_h \left( \frac{2\pi}{\omega} \right) - \oint \int_0^L 2\pi r_2 q_2'' dy dt \end{aligned} \quad (6)$$

Equation 6 shows that the enthalpy difference over the control volume is equal to the heat transfer at the control volume surface. The heat flux from the heater to control volume is constant. But the heat flux from the glass wall to the environment is not constant; it varies with position and time. The last term on the right hand side of 6 shows the heat loss from the glass tube surface to the environment. The total heat loss over a cycle can be calculated by means of 6 as follows.

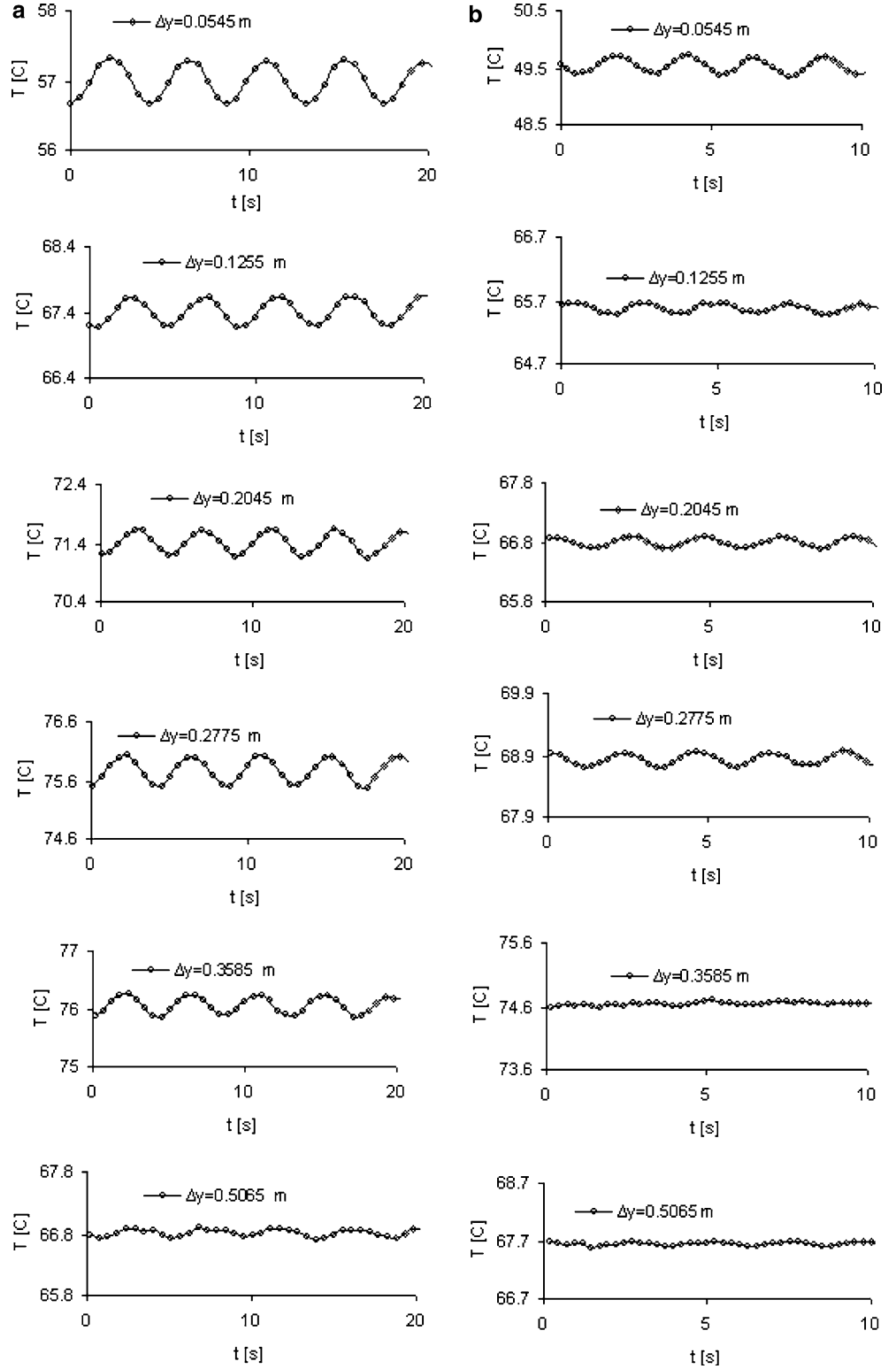
$$Q_k = \oint \int_0^L 2\pi r_2 q_2'' dy dt = q_1'' 2\pi r_1 l_h \left( \frac{2\pi}{\omega} \right) - (H_2 - H_1) \quad (7)$$

In this equation, the terms except heat loss term are calculated from experimental data.

It is clear that the surface temperatures of the inner side of the glass tube should vary harmonically with time. The variation of the measured surface temperatures of the outer side of the glass tube with time can be neglected as observed in the experiments. Although, outer surface temperatures have a negligible harmonic oscillation, it can be attributed to the damping effect of the glass wall.

The averaged surface temperature of the outer side of glass tube can be calculated from the measured values and it can be separated into two regions corresponding to the water and air regions with respect to the oscillation axis  $z_0$ . Thus, by using these averaged outer surface

**Fig. 3** Heater surface temperatures versus time ( $x_m=0.125$  m,  $q_e=100$  W,  $z_0=0.625$  m,  $\Delta y$ , distance from initiative of heater).  
**a**  $\omega=1.435$  rad/s.  
**b**  $\omega=2.723$  rad/s



temperatures, the heat loss can be determined and separated into two parts approximately as follows by considering the Newton's cooling law.

$$\frac{Q_{kl}}{Q_k} = \frac{z_0(T_{cl} - T_a)}{z_0(T_{cl} - T_a) + (L - z_0)(T_{ca} - T_a)} = \phi \quad (8)$$

$$\frac{Q_{ka}}{Q_k} = \frac{(L - z_0)(T_{ca} - T_a)}{z_0(T_{cl} - T_a) + (L - z_0)(T_{ca} - T_a)} = (1 - \phi) \quad (9)$$

The thermal energy conservation equation for water region over a cycle without flat interface simplification can be written as follows.

**Fig. 4** Time-averaged heater surface temperatures versus position and frequency  $q_e = 100$  W, (Experiments 5–8, see Table 1)

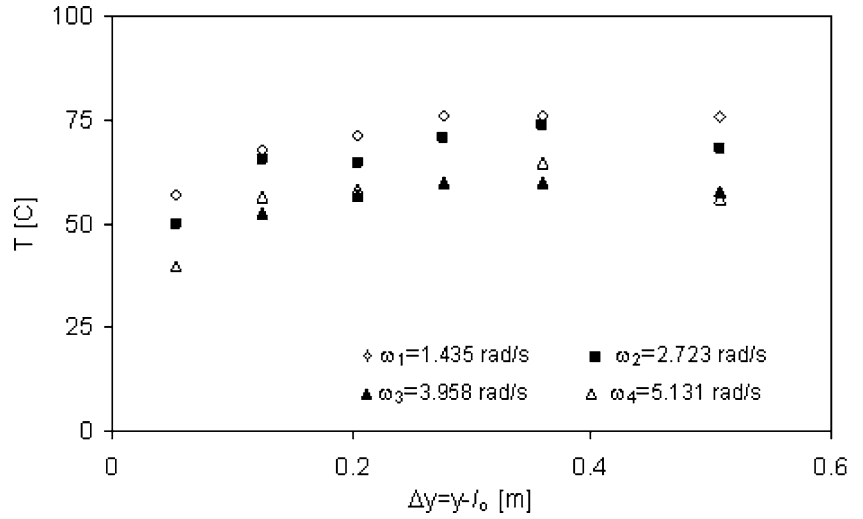
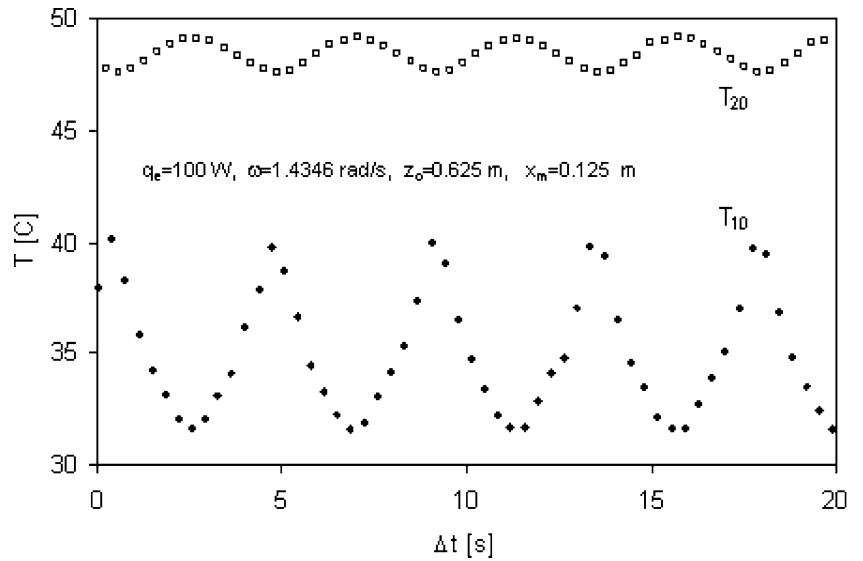


**Fig. 5** Area-averaged probe temperature versus relative time



$$H_1 = \oint_0^z 2\pi r_2 q_2'' dy dt - \oint_{l_0}^{y^*} 2\pi r_1 q_1'' dy dt \quad (10)$$

Here,  $y^*$  is the distance from reference to the meniscus. The first term on the right side of this equation shows the heat loss from the water side of the glass tube to the environment, so that the Eq. 10 can be rearranged as

$$Q_l = \oint_{l_0}^{y^*} 2\pi r_1 q_1'' dy dt = Q_{kl} - H_1 \quad (11)$$

Substituting 7 and 8 in the 11, the heat transfer to the water from the heater over a cycle is determined as

$$Q_l = m_l q_1'' 2\pi r_1 l_h \left( \frac{2\pi}{\omega} \right) - \phi H_2 - (1 - \phi) H_1 \quad (12)$$

Cycle-averaged experimental data are given in the Table 1 with respect to the frequencies and the heater power.

### 3.4 Prediction of Nusselt number

The total heat transfer to the water over a cycle  $Q_l$  can be written as follows

$$Q_l = 2\pi r_1 l_h h (T_{w0} - T_0) (2\pi/\omega) \quad (13)$$

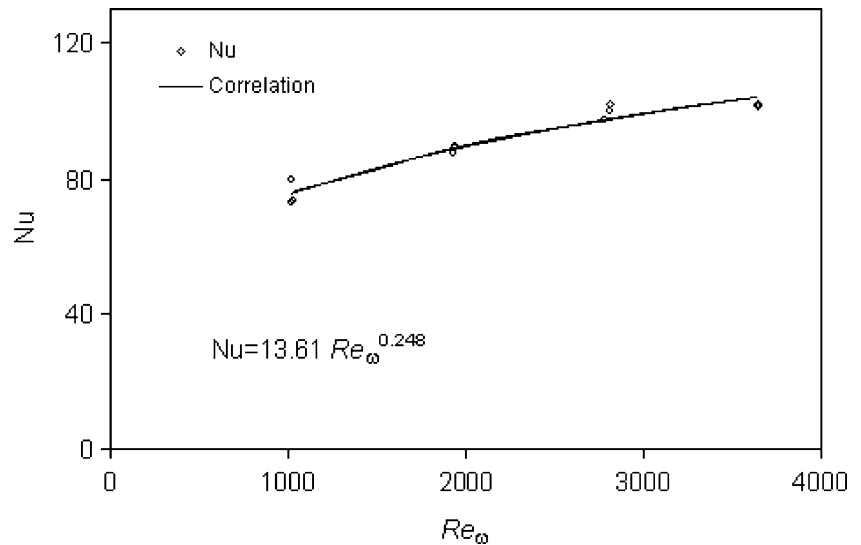
Here, the averaged water temperature can be defined as

$$T_0 = \frac{T_{10} + T_{20}}{2} \quad (14)$$

$T_{10}$  and  $T_{20}$  represent time-averaged probe temperatures as given in Table 1. Considering 13, the Nusselt number is defined as

**Table 1** Cycle-averaged experimental data

	$\omega$ (rad/s)	$Re_\omega$	$q_e$ (W)	$T_{w0}$ (C)	$T_{20}$ (C)	$T_{10}$ (C)	$\phi$	$-H_1$ (J)	$H_2$ (J)	$Q_k$ (J)	$Q_l$ (J)	$h$ (W/m <sup>2</sup> -K)	$Nu$
Exp-1	1.445	1026.1	50	41.7	36.2	27.6	0.767	126.91	0.14	90.37	196.19	80.83	73.71
Exp-2	2.712	1926.0	50	34.8	29.9	25.0	0.746	71.42	0.08	44.34	104.49	95.99	87.53
Exp-3	3.906	2773.7	50	30.0	27.0	24.2	0.753	50.65	0.06	29.72	73.02	106.50	97.12
Exp-4	5.131	3642.9	50	29.5	25.1	25.3	0.802	47.87	0.03	13.34	58.57	111.19	101.38
Exp-5	1.435	1018.7	100	54.6	48.0	34.8	0.765	182.22	0.17	255.59	377.68	87.22	79.53
Exp-6	2.723	1933.4	100	49.9	43.2	32.2	0.773	157.77	0.15	72.86	214.07	98.52	89.84
Exp-7	3.948	2803.5	100	43.4	35.9	30.6	0.794	82.38	0.05	76.72	143.34	109.62	99.96
Exp-8	5.131	3642.9	100	40.9	32.8	30.5	0.791	57.98	0.03	64.47	109.00	112.05	102.17
Exp-9	1.434	1018.3	150	68.9	59.4	41.4	0.783	348.76	0.47	308.01	590.00	80.25	73.18
Exp-10	2.723	1933.4	150	57.7	47.3	37.5	0.790	201.11	0.21	144.83	315.46	97.54	88.95
Exp-11	3.958	2810.6	150	52.0	40.1	36.1	0.795	150.14	0.07	87.91	220.05	111.86	102.00
Exp-12	5.131	3642.9	150	50.2	35.4	34.8	0.817	132.42	0.01	51.29	174.35	112.04	102.17

**Fig. 6** Nusselt number versus kinetic Reynolds number

$$Nu = \frac{hl_h}{k} = \frac{l_h}{k} \frac{Q_l}{2\pi r_1 l_h (T_{w0} - T_0) (2\pi/\omega)} \quad (15)$$

The calculated Nusselt numbers using 15 are given in Table 1 with respect to the frequencies and the heater power.

Nusselt number can be written as a function of kinetic Reynolds number  $Re_\omega = \omega d^2/\nu$ , dimensionless oscillation amplitude  $A_o = 2x_m/d$ , the length to diameter ratio of the heater  $d/l_h$  and Prandtl number [8].

$$Nu = f(Re_\omega, A_o, d/l_h, Pr)$$

In this study, only kinetic Reynolds number is variable so that the correlation equation for Nusselt number is found as

$$Nu = 13.61 Re_\omega^{0.248} \quad (16)$$

and this equation is valid in the following range of kinetic Reynolds number.

$$1000 < Re_\omega < 4000$$

The graphical representation of 16 is shown in Fig. 6 together with the experimental data.

### 3.5 Uncertainty analysis

An uncertainty analysis based on the method described by Holman [11] is performed. The uncertainty in the experimental data can be considered by identifying the main sources of errors in the measurements. The main source of errors in reported results on the Nusselt number are statistical uncertainty power input, heater surface mean-temperatures and bulk temperature of fluid.

Prior to the experiments all thermocouples were calibrated in a constant temperature bath (K type, Omega) to ensure the accuracy of  $\pm 0.1^\circ\text{C}$ . The voltage input to the electric heater is measured with sensitivity of  $\pm 1$  V and accuracy of 1 percent. The calculated power output uncertainty is less than 4. Oscillation frequency of the water column is equal to that of the motor drive and is measured by a tachometer within a 0.5% error in terms of the frequency measurement. The estimated uncertainties in the power output, heater surface mean-temperature and bulk-temperature of fluids are 6.2, 1.34 and 0.35, respectively. Finally, the largest uncertainties of the Nusselt numbers were computed to be about  $\pm 10.6\%$ , by using the uncertainty estimation method of Holman [11].

---

#### 4 Conclusion

In this study, the heat transfer from a heated surface to an oscillating vertical annular liquid column having an interface with the atmosphere is investigated experimentally. The experiments are carried out for different frequencies while the displacement amplitude remains constant for all cases considered. All the mathematical calculations in analyzing the experimental data are based on measurements taken from the test section considered as the control volume shown in Fig. 2. A correlating equation for cycle-averaged Nusselt number has been obtained from the experimental data. The prediction of the cycle-averaged Nusselt number with respect to kinetic Reynolds number is shown to be in good agreement with the experimental data.

**Acknowledgements** The present work was supported by ITU Institute of Science and Technology. Thesis support number : 1969.

---

#### References

1. Chatwin PC (1975) On the longitudinal dispersion of passive contaminant in oscillatory flows in tubes. *J Fluid Mech* 71(3):513–527
2. Watson EJ (1983) Diffusion in oscillatory pipe flow. *J Fluid Mech* 133:233–244
3. Kurzweg UH, Zhao LD (1984) Heat transfer by high-frequency oscillations: A new hydrodynamic technique for achieving large effective thermal conductivities. *Phys Fluids* 27(11):2624–2627
4. Zhang JG, Kurzweg UH (1990) Numerical simulation of time-dependent heat transfer in oscillating pipe flow. *J Thermophys* 5:401–406
5. Ozawa M, Kawamoto A (1991) Lumped-parameter modeling of heat transfer enhanced by sinusoidal motion of fluid. *Int J Heat Mass Trans* 34(12):3083–3095
6. Zhao TS, Cheng P (1998) Heat transfer in oscillatory flow. *Annual review of heat transfer, Vol.IX*, Chapter 7, The Hong Kong University of Science & Technology. Clear Water Bay, Kowloon, Hong Kong
7. Zhao TS, Cheng P (1995) A numerical solution of laminar forced convection in a heated pipe subjected to a reciprocating flow. *Int J Heat Mass Trans* 38(16):3011–3022
8. Zhao TS, Cheng P (1996) Oscillatory Heat transfer in a pipe subjected a periodically reversing flow. *ASME J Heat Trans* 118:592–598
9. Tang X, Cheng P (1993) Correlations of the cycle-averaged Nusselt number in a periodically reversing pipe flow. *Int Comm Heat Mass Trans* 20:161–172
10. Chen ZD, Chen JJJ (1998) A simple analysis of heat transfer near an oscillating interface. *Chem Engng Sci* 53(5):947–950
11. Holman JP (2001) *Experimental methods for engineers*. McGraw-Hill, New York